KERNFORSCHUNGSANLAGE JÜLICH GmbH
Institut für Plasmaphysik
Association EURATOM-KFA

The ECE Diagnostik System on TEXTOR

by
G. Waidmann

Jül - 1898
Februar 1984
ISSN 0366-0885

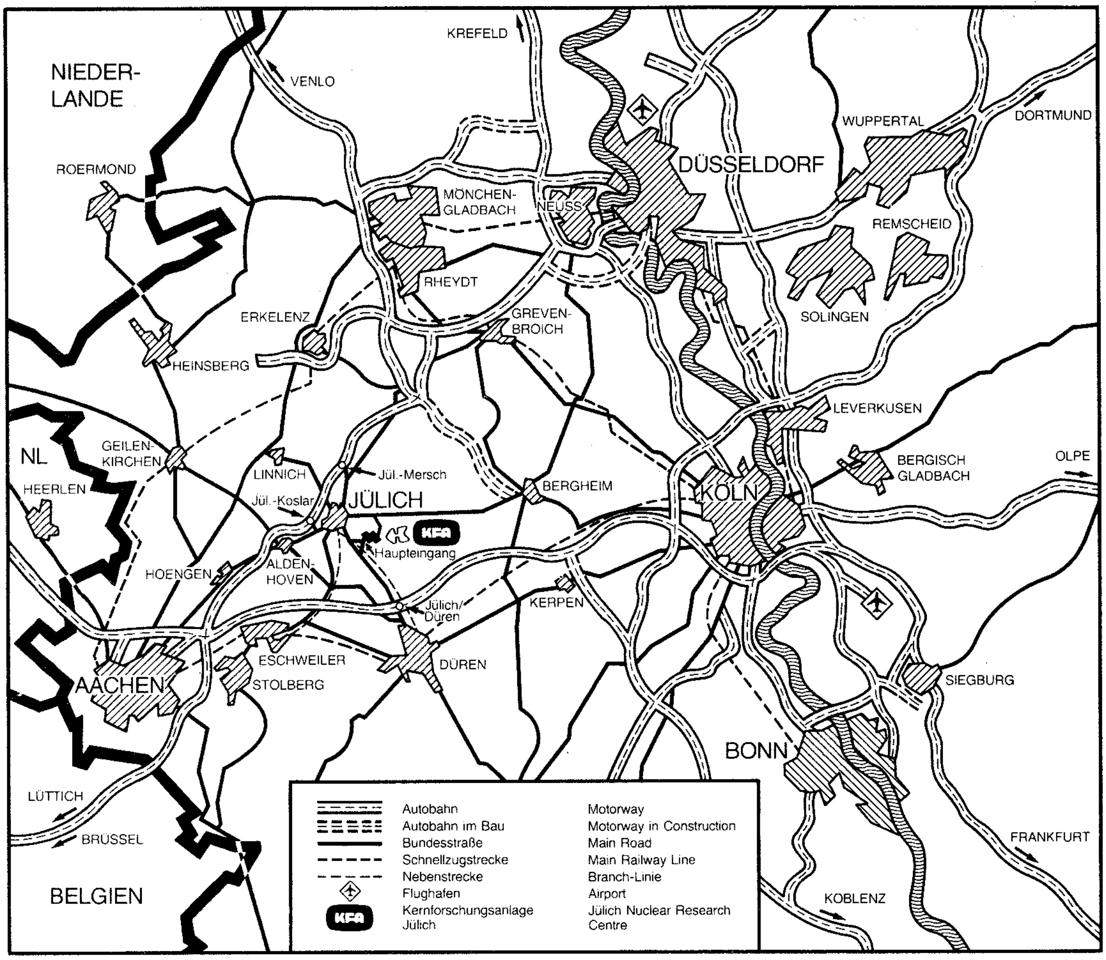

Als Manuskript gedruckt

Berichte der Kernforschungsanlage Jülich – Nr. 1898
Institut für Plasmaphysik Jül - 1898

Zu beziehen durch: ZENTRALBIBLIOTHEK der Kernforschungsanlage Jülich GmbH
Postfach 1913 · D-5170 Jülich (Bundesrepublik Deutschland)
Telefon: 02461/610 · Telex: 833556 kfa d

The ECE Diagnostik System on TEXTOR

by
G. Waidmann

The ECE Diagnostic System on TEXTOR

Abstract

A heterodyne millimeter wave radiometer was built to record simultaneously the first ordinary and second extraordinary wave of ECE emitted from the same point in the plasma. The optical depth of the TEXTOR plasma was calculated for typical TEXTOR parameters. The accessibility of ECE-radiation was considered. First experimental results from TEXTOR are presented. The electron temperature on axis of the TEXTOR plasma is routinely monitored from ECE intensity measurements. An instantaneous half electron temperature profile and its development in time are shown. Internal plasma disruptions are visualized by a sawtooth modulation of the ECE intensity. Also MHD-activity in the plasma is reflected in the ECE.

Contents

1. Introduction

The electron cyclotron resonance radiation emitted from the TEXTOR plasma is under certain plasma parameter conditions a black body radiation. A numerical parameter study was carried out to evaluate the optical thickness of the TEXTOR plasma for typical operation conditions. The absorption power was calculated for the two lowest cyclotron harmonics using theoretical expressions of Bornatici /1/ as a function of the radial position in the plasma for various temperature and density profiles. With the exception of the plasma boundary zones the emission originates from an optically thick plasma.

The continuous acquisition of the electron temperature with good spatial resolution represents a most valuable monitor for the general plasma performance. A continuous information about the electron temperature profile is required to study transport and plasma stability phenomena in critical parameter regimes.

2. Cyclotron Emission and Accessibility of Radiation

The specific intensity radiated from the region around cyclotron resonance is given for a thermal plasma /1/ as

$$\delta I_n^{(i)}(\omega) = \frac{\omega^2 k T_e(r)}{8\pi^3 c^2}\left[1 - e^{-\tau_n^{(i)}}\right]$$

n = 1,2,.... harmonic of $\omega_{c(r)}$

i = 0 ordinary wave with $E \parallel B$

i = x extraordinary wave with $E \perp B$

τ_n = optical thickness

For blackbody emission, where $\tau_n \gg 1$, the specific intensity is proportional to the local electron temperature $T_e(r)$ and allows a continuous electron temperature measurement if the ECE radiation is accessible. The electron temperature should stay in the range of the "low" temperature, local approximation /1/ and the electron velocity distribution function be Maxwellian.

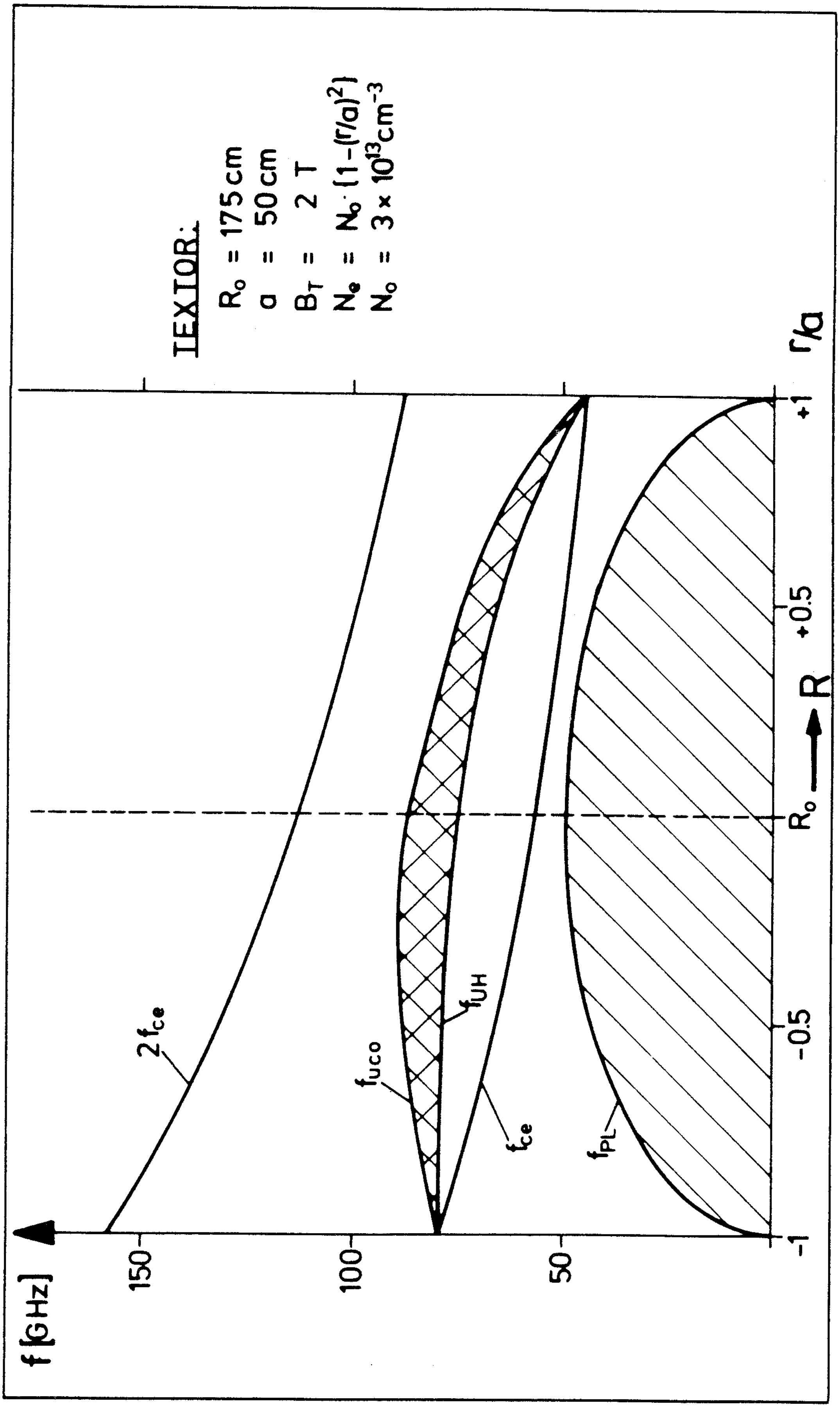

Fig. 1 Characteristic Frequencies of the TEXTOR Plasma.

The characteristic frequencies for a typical TEXTOR plasma are shown in Fig. 1. A parabolic density profile $N_e = N_o \cdot [1 - (r/a)^2]$ and a temperature profile $T_e(r) = T_o \cdot [1 - (r/a)^2]^2$ were assumed. The plasma frequency f_{PL}, the first and second cyclotron harmonic f_{ce} and $2f_{ce}$ are shown over the plasma diameter. Included are also the upper hybrid and the cyclotron cut-off frequencies. As long as the plasma frequency stays far enough below the f_{ce}-line, the first harmonic is accessible from the high- and low field side of the machine. The extraordinary, second harmonic frequency is not impeded by absorption or reflection for TEXTOR parameters envisaged at present.

3. Optical Thickness of the Plasma

A convenient situation is found for optically thick plasmas when $\tau_n \gg 1$. The theory for the optical thickness has been developed recently for plasmas with spatially variable magnetic field for the two fundamental modes with wave propagation perpendicular to the magnetic field B_o and scale length $L \gg |\frac{2\pi}{k}|$ (see e.g. /1/). For the extraordinary, n-th harmonic one finds

$$\tau_n^{(x)} = \frac{\pi^2 n^{2(n-1)}}{2^{n-1}(n-1)!} <A_n> \left(\frac{\omega_p}{\omega_c}\right)^2 \left(\frac{V_t}{c}\right)^{2(n-1)} \frac{L_B}{\lambda_o}$$

and for the ordinary wave

$$\tau_n^{(o)} = \frac{\pi^2 n^{2(n-1)}}{2^{n-1}(n-1)!} \left(1 - \frac{\omega_p^2}{n^2 \omega_c^2}\right)^{n-1/2} <D_n> \left(\frac{\omega_p}{\omega_c}\right)^2 \left(\frac{V_t}{c}\right)^{2n} \frac{L_B}{\lambda_o}$$

Fig. 2 shows for the extraordinary, second harmonic wave and TEXTOR parameters the absorption power $A = 1 - e^{-\tau_2^{(x)}}$ versus plasma diameter. The peak electron temperature $T_e(Ro)$ is plotted as curve parameter between 0.25 and 3 keV. For temperatures of $T_e(Ro) = 1$ keV the major part of the plasma cross section is optically thick. Fig. 3 shows in an analog plot the absorption power $A = 1 - e^{-\tau_1^{(o)}}$ for the first harmonic ordinary wave. The optical thickness is not as good as that for the extraordinary wave but reaches in the central part for TEXTOR electron temperatures also blackbody emission. The trade-off between electron density and electron temperature to reach $\tau_2^{(x)} = 1$ is demonstrated in Fig. 4. The plasma parameters T_e and n_e have to stay above the shaded area (s. appendix).

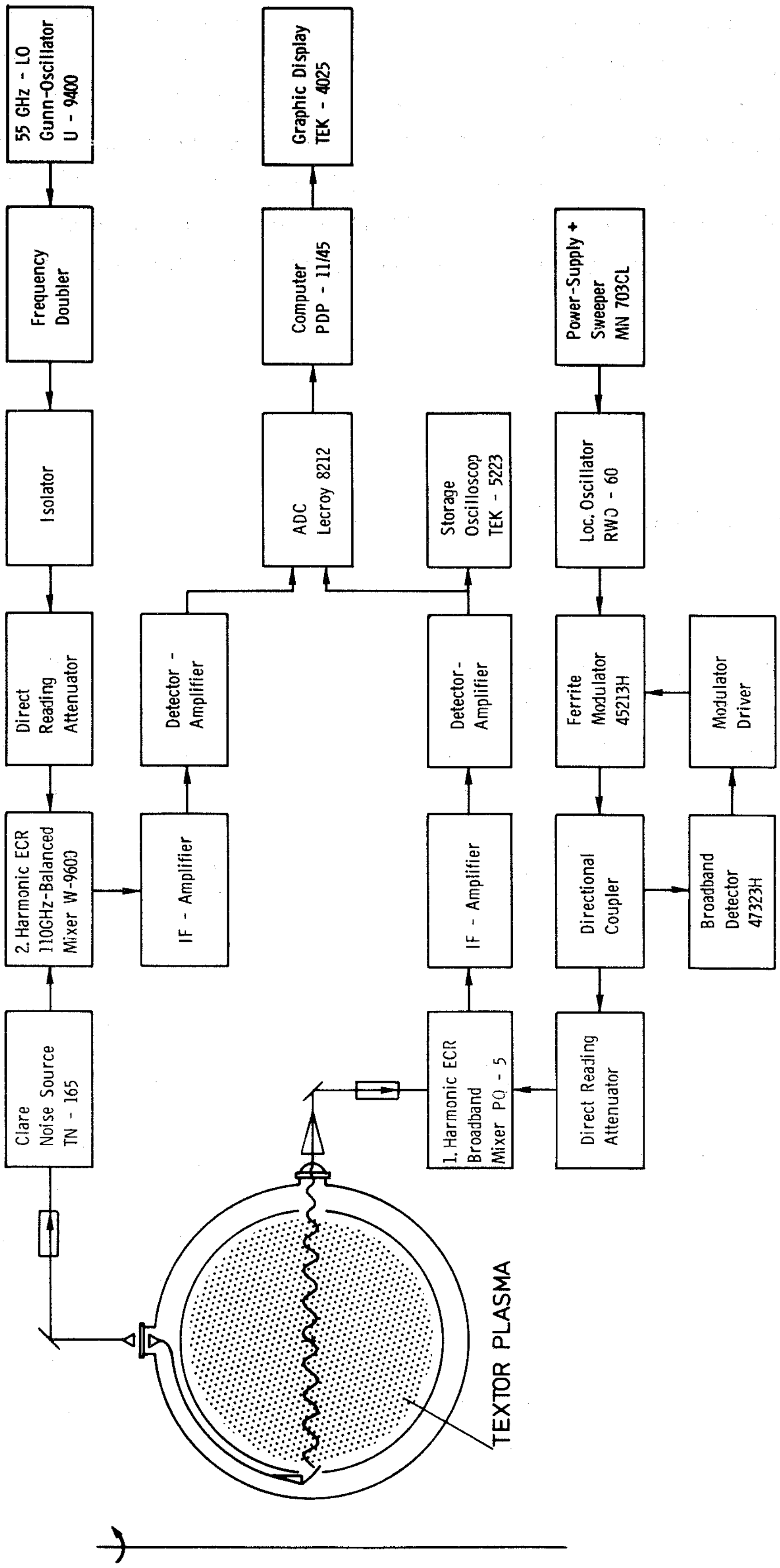

Fig. 5 Schematic diagram of the heterodyne radiometer for the first and second harmonic of ECE.

4. The MM-Wave Radiometer System

4.1 Experimental Arrangement

A heterodyne receiver system for the first and second harmonic is shown schematically in Fig. 5. Similar systems have been described in the literature /4 – 6/. A parabolic antenna on the high field side mounted inside the vacuum vessel and a pyramidal horn antenna outside the vessel on the low field side allow to receive the ECE radiation from the same source point. This antenna configuration allows a millimeter wave transmission experiment to check the condition of optical thickness. Bakeable aluminum oxide windows /7/ permit a low loss transit of the ECE through the hot vessel wall.

The receiver part for the ordinary, first harmonic is a broadband system and can be tuned electrically to any radial position between R_o and $R_o + a$ or swept through periodically in 10 msec time intervalls. A broadband balanced mixer PQ-5 with a noise figure of 6dB DSB together with a sweepable local oscillator RWO-60 permitts an ECE scan over the plasma radius. Using a fixed frequency local oscillator (e.g. Gunn-oscillator)a system sensitivity of $S_l^{\cdot}=-78$ dBm was evaluated. The resolution bandwidth under these conditions was $\Delta f = 500$ MHz. The sensitivity is considerably lower for a swept mode broadband application. The system noise figure increased to NF $\geqslant 20$ dB because of noise generated in the backward wave local oscillator. The radial resolution is $\Delta R = 3$ cm taking into account the IF-bandwidth and the DSB property of the mixer.

The receiver for the extraordinary, second harmonic was operated with a balanced mixer TRG-W9600 with GaAs – Schottky barrier beam lead diodes and a frequency doubled Gunn-oscillator. That system yielded a sensitivity of $S_2=-71$ dBm. Both receivers showed nearly identical experimental results. The radiometer system was placed 5 m away from the center of the machine in order to avoid magnetic interference with electronic components. The distance from the pick-up antennas to the receivers was bridged by means of overdimensional waveguides WR 90 using quasioptical transmission techniques. After carefully tapering down from WR 90 standard waveguides WR 19 respectively WR 10 were used for the other system components. The two receiver systems are interfaced to the TEXTOR diagnostics data acquisition system /8/.

The radiometer was calibrated in situ for electron temperature measurements by a Thomson scattering technique.

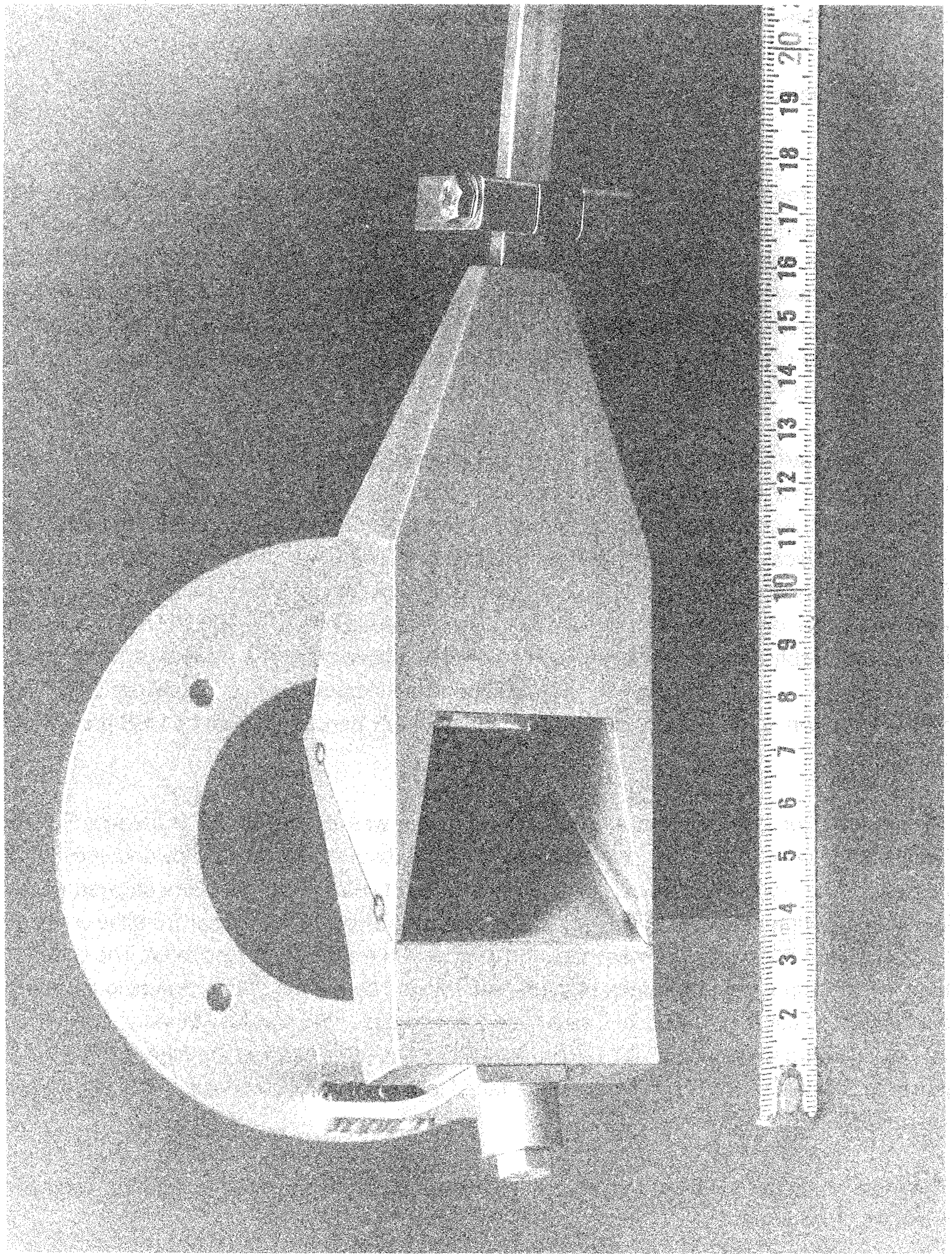

Fig. 6 A parabolic antenna mounted inside the vacuum vessel to pick-up ECE from the high magnetic field side.

4.2 **System Components**

4.2.1 Antennae

The receiving antennae were specially built for the TEXTOR requirements /9/ by spark erosion technique. In order to receive the ECE from the high field side a flat aerial had to be mounted between liner and vacuum vessel wall in the equatorial plane looking in radial direction towards the plasma center. A flat parabolic antenna (s. Fig. 6) machined out of stainless steel was mounted into a bucket of the vacuum vessel. The antenna gain was evaluated to G = 25 dB. Also stainless steel waveguides were used to transfer the received ECE to a ceramic window where it was handed over to the overdimensional transmission system.

The receiving antenna for the low field side was machined out of brass and has a gain of 30 dB. It is mounted outside the vacuum system in the equatorial plane.

4.2.2 Heterodyne Mixers

The ECE radiation is frequency downconverted by low-noise Schottky mixers. Balanced mixers employing strip line technique are used to reduce L.O.-noise. Preamplifiers with 20 dB gain are integrated with the balanced mixers. Postamplifier and audioamplifier add a future gain of 40 dB. The postamplifier consists of two amplifier modules with an IF-bandpass of 100-500 MHz. The bandpass of the amplifier is tailored to that of a tunnel diode video detector. For fixed frequency operation narrow band Gunn oscillators (L = 20 mW) with selectable frequency are choosen. Their frequency determines the position of radiation emission detected from the plasma. For scanning operation an electronically tunable backward wave oscillator RWO-60 was used. The system noise figure and the receiver sensitivity were determined using standard noise measurement procedures. Noise tubes (C.P. Claire TN-165 resp. TN-163) were incorporated into the signal waveguides. The noise figure was measured utilizing the ON-OFF method by the relation

$$NF = ENR - 10 \log \frac{P_{ON} - P_{OFF}}{P_{OFF}}$$

with ENR the excess noise ratio of the standard noise tube.

A clear deterioration of the noise figure of a heterodyne mixer was observed during a plasma shot which developed into a hard run-away discharge. The mixers were capsuled therefore by a 3 cm lead shield to avoid hard x-ray damage.

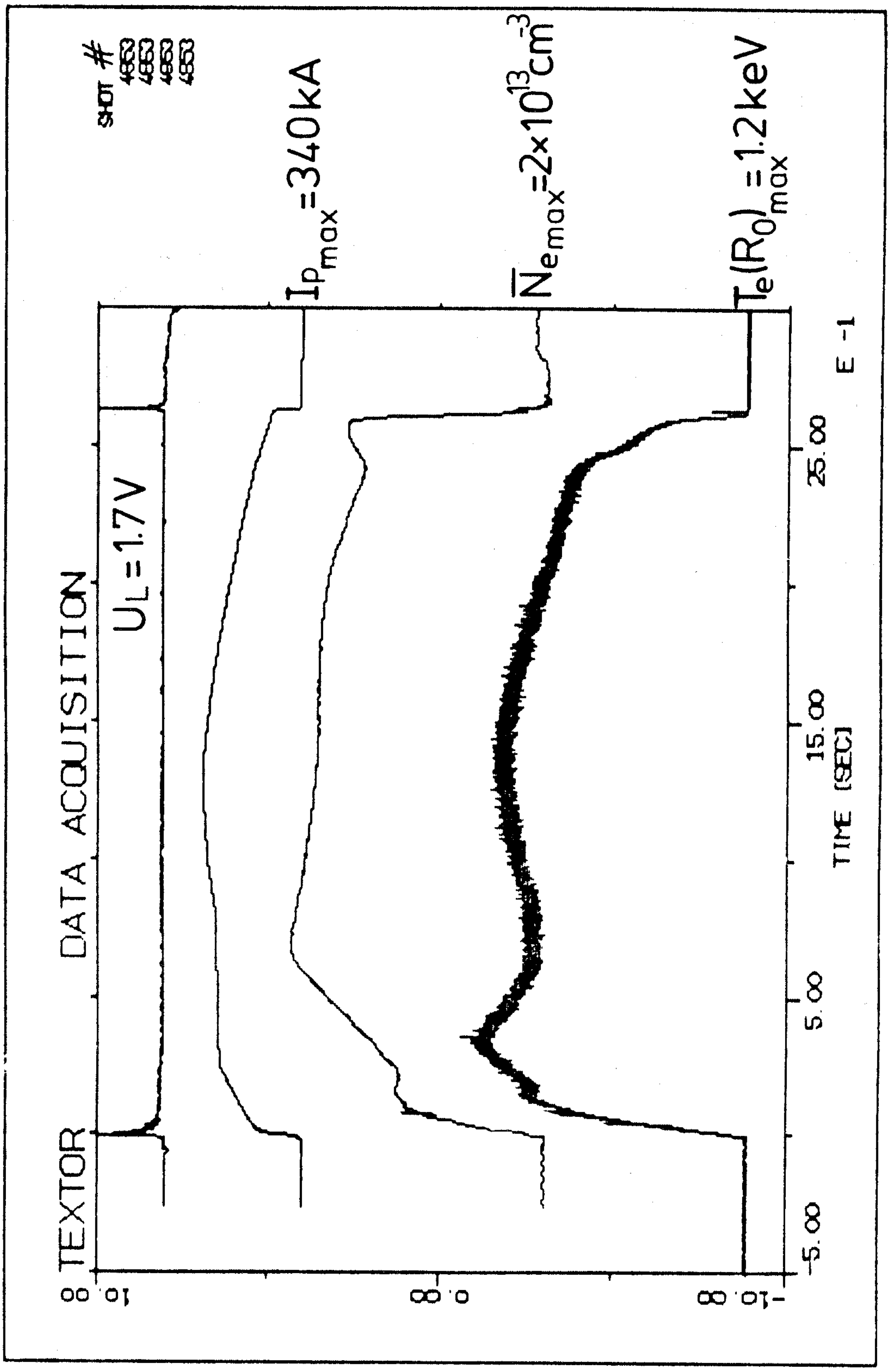

Fig. 7 Time dependence of the loop voltage U_L, plasma current I_p, average electron density $\bar{N}_e$ and electron temperature on axis $T_e(R_0)$ for a typical TEXTOR discharge.

5. Experimental Results

5.1 Electron temperature measurement

A millimeter wave transmission test was carried out for the first harmonic wave of ECE. Over the antenna system described an ordinary EM-wave corresponding to $\omega_c \equiv \omega_c (R_0)$ was transmitted through the vessel in the equatorial plane. The absorption of the wave was observed during the plateau phase of the discharge and the optical thickness $\tau_1^{(o)} > 1$ was ascertained.

A typical TEXTOR discharge is shown in Fig. 7. The time dependence of the loop voltage U_L, the plasma current I_p, the average electron density $\bar{N}_e$ and the electron temperature on axis $T_e(R_0)$ are plotted for a discharge with pure Ohmic heating. In the current plateau phase the electron temperature on axis shows a complementary behaviour to the average electron density. A peak temperature of $T_e (R_0) = 1.2$ keV was measured early in the plateau phase. For a comparison the first harmonic ordinary $T_{e1}(R_0)$ and the second harmonic extraordinary wave $T_{e2}(R_0)$ are shown for the same shot in Fig. 8. Nearly identical results are obtained. A half electron temperature profile was obtained with the fixed frequency first harmonic radiometer by means of a small variation of the toroidal magnetic field. The profile was constructed from 16 consecutive shots (s. Fig. 9). An assumed temperature profile $T_e(R) = T_e(R_0)\, x[1-(r/a)^2]^2$ fitted at the center $R = R_o$ is also included.

The time behaviour of the electron temperature profile was observed with the scanning radiometer /10/. In Fig. 10 the output of the fixed frequency radiometer and the scanning radiometer are demonstrated for TEXTOR shot # 4855. Fig. 11 shows the profile behaviour in time.

5.2 Instabilities monitored by ECE

The ECE-radiation from the plasma center is a sensitive monitor for general plasma performance. Under certain operation conditions the ECE-intensity reveals a fine structure (s. Fig. 12). Sawtooth like oscillations modulate the radiation intensity and signal that internal disruptions begin (s. Fig. 13). These internal disruptions affect the central part of the discharge and level the temperature profile within the $q = 1$ surface. The oscillation period was observed to increase with electron density and exceeded 10 msec in some cases. The appearance of sawtooth oscillations indicates a plasma state which is favourable for additional heating, e.g. ICRF.

The deveolopment of a disruptive discharge is demonstrated in Fig. 14. The lower curve shows the growth of an $M = 2$ instability. After a certain development time of $M = 2$ minor disruptions are visible as tiny negative voltage spikes in the loop voltage. The ECE intensity decays with the

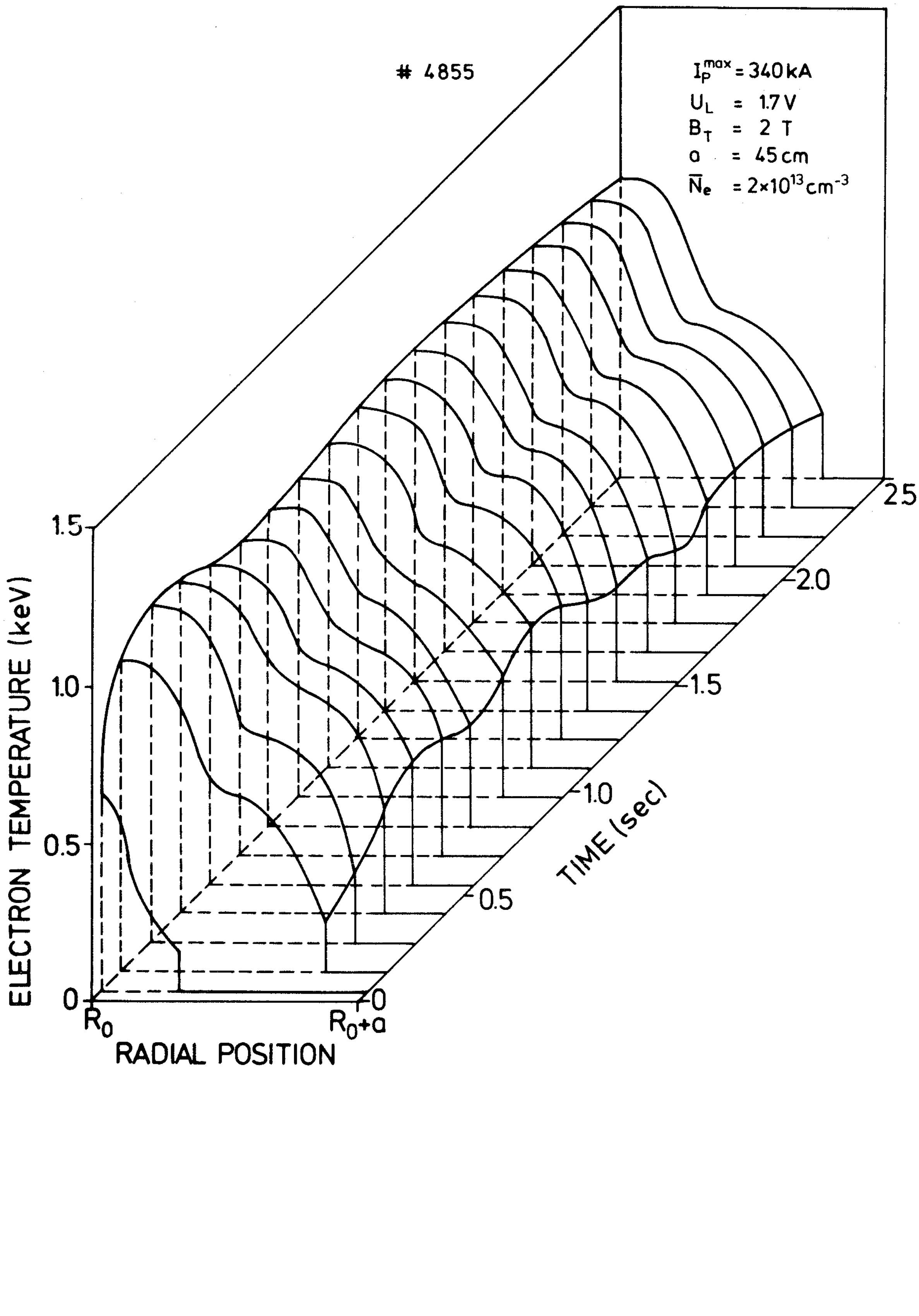

Fig. 11 Electron temperature profile (# 4855) obtained with the scanning radiometer.

development of the M = 2 instability and precursors of disruptive energy loss in the central part of the plasma appear. No change in plasma current is observed so far. After a drastic change in the rotation frequency of the M = 2 mode the first steep negative voltage spike occurs and positive plasma current pips show up. Deep dips in the ECE emission indicate a strong loss of plasma energy and the plasma current column starts to tumble. These major disruptions repeat and the plasma current begins to fall. After 5 consecutive disruptions the plasma column shows already a strong displacement towards the inside limiter and a hard disruption terminates the plasma current.

Already in the current rise phase a marked dip in ECE was seen. The dip signals the transit of the rational $q(a) = 6$ surface when passing across the limiter position in TEXTOR. Fig. 15 shows a similar current rise phase with beginning M = 2 activity but the mode was choked by gas influx. The decay in ECE-radiation stops, the central electron temperature recovers and a longlasting discharge was achieved.

Under low density discharge conditions nonthermal ECE signals were observed. (s. Fig. 16). Bursts of radiation spikes are superimposed on the normal emission intensity. The emission of radiation spikes is explained as an instability of a runaway electron beam in the plasma. The experimental observation resembles the theoretical picture given by Parail and Pogutse /11/ for a kinetic instability in a low density tokamak plasma for the condition $\omega_{ce} > \omega_{pe}$. In their model a conversion of longitudinal into transversal electron energy takes place accompanied by the emission of a plasmon. Further identification of this instability requires a parameter study of electron density and toroidal magnetic field on the shape and repetition rate of the emission spikes. Typical emission spikes are shown in Fig. 17, an enlarged display of Fig. 16. This anomalous emission disappears again at higher electron densities.

The author would like to thank Drs. E. Graffmann and J. Schlüter for their temperature calibration data, Dr. M. Korten and the data acquisition group for their help and Mr. W. Pysik for many technical contributions.

6. References

/1/ Bornatici, M., Cano, M., de Barbieri, O., Engelmann, F.
Nuclear Fusion **23**, 9 (1983) p. 1153

/2/ Engelmann, F. Curatolo, M.
Nuclear Fusion **13** (1973) p. 497

/3/ Bornatici, M.
Plasma Physics, **24**, 6, p. 637 (1982)

/4/ Cano, R., Bagdasarov. A.A., Strelkov, A.B., Gorbunov, E.P.
Rep. EUR-CEA-FC-989, Dec. (1978)

/5/ Efthimion, P.C., Arunasalam, V., Bitzer, R., Campbell, L., Hosea, J.C.
Rev. Sci. Instrum. **50**, 8, p 949, Aug. (1979)

/6/ Hosea, J., Arunasalam, V., Cano, R.
Phys. Rev. Lett. **39**, 7 (1977), 408

/7/ Hüttemann, P.W., Waidmann, G.
Rep. KFA-Jül-1802, Sept. 1982

/8/ Korten M.
12th Symp. on Fusion Technology, Jülich 1982, paper E 30

/9/ Conrads, H.
10th Symp. on Fusion Technology, Padua 1978, paper A1

/10/ Waidman, G.
11th Europ. Conf. on Controlled Fusion and Plasma Physics, Aachen Sept. 1983, p. 104

/11/ Parail, V.V., Pogutse, O.P.
Sov. J. Plasma Phys. **2**, No. 2, March-April 1976, p. 125 ff.

7. Figure Appendix

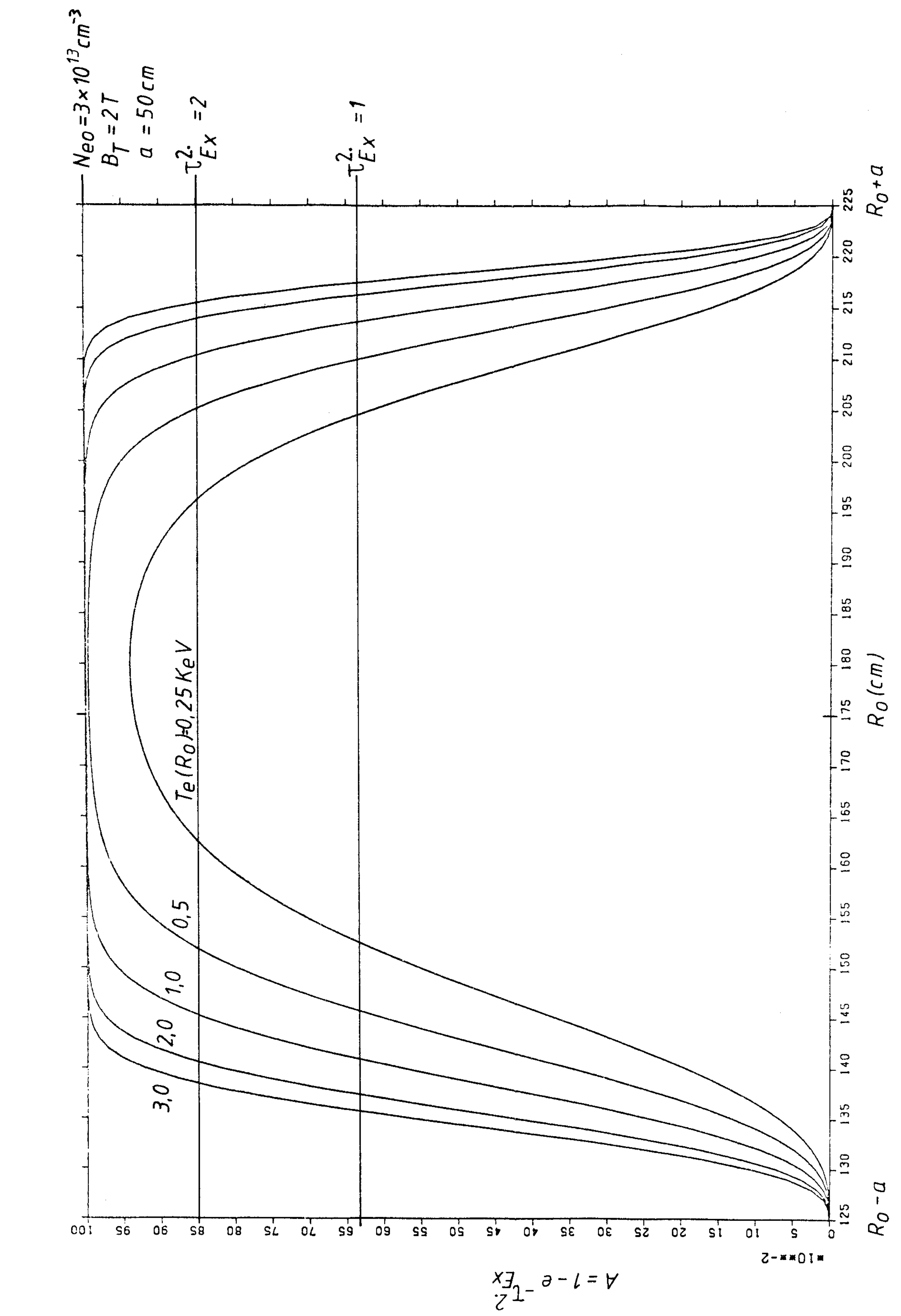

Fig. 2 Absorption power of the second harmonic extraordinary wave versus plasma radius for assumed typical TEXTOR parameters.

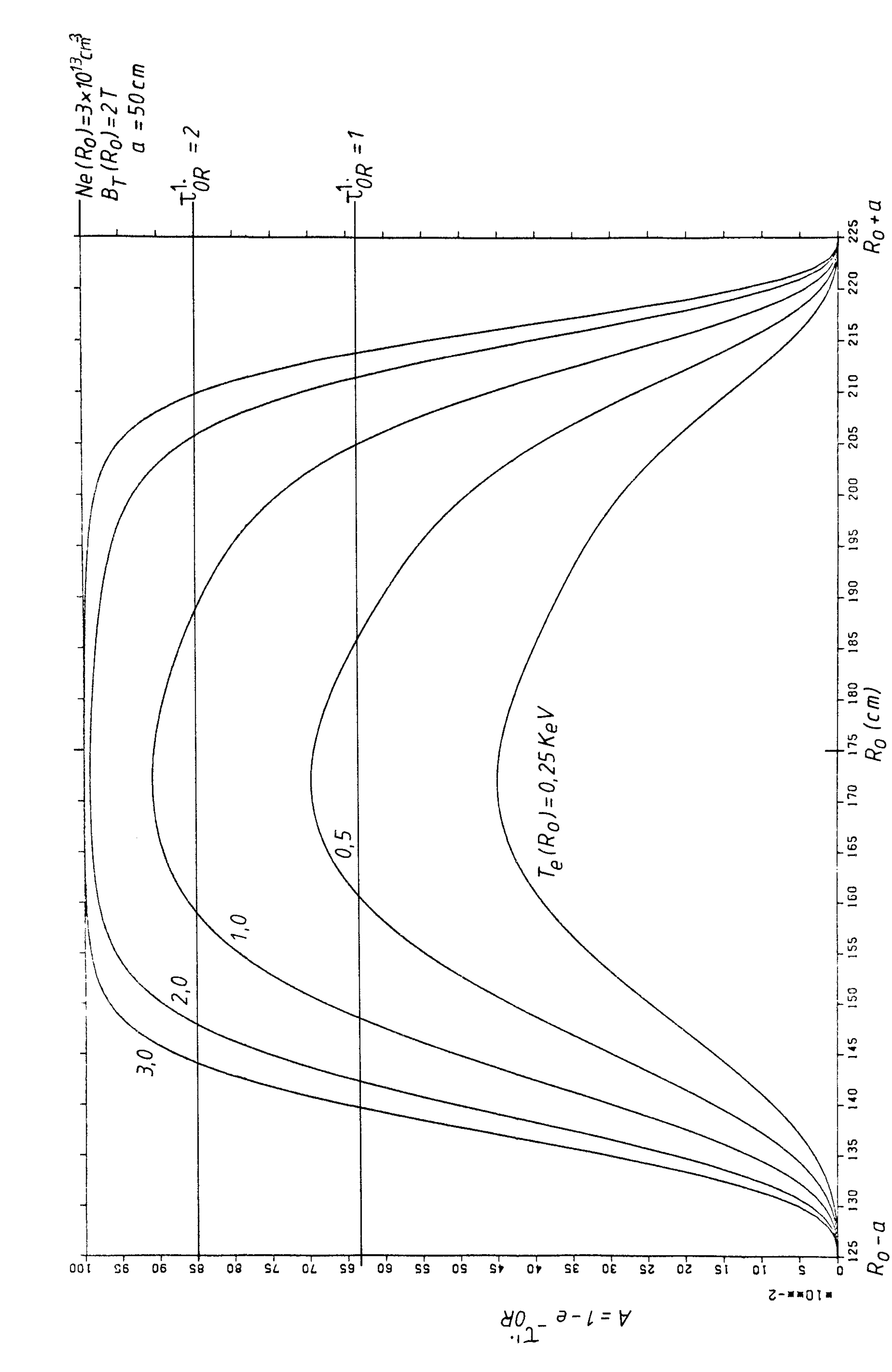

Fig. 3 Absorption power A = 1-e $-\tau_1^{(o)}$ of the first harmonic ordinary wave versus plasma radius.

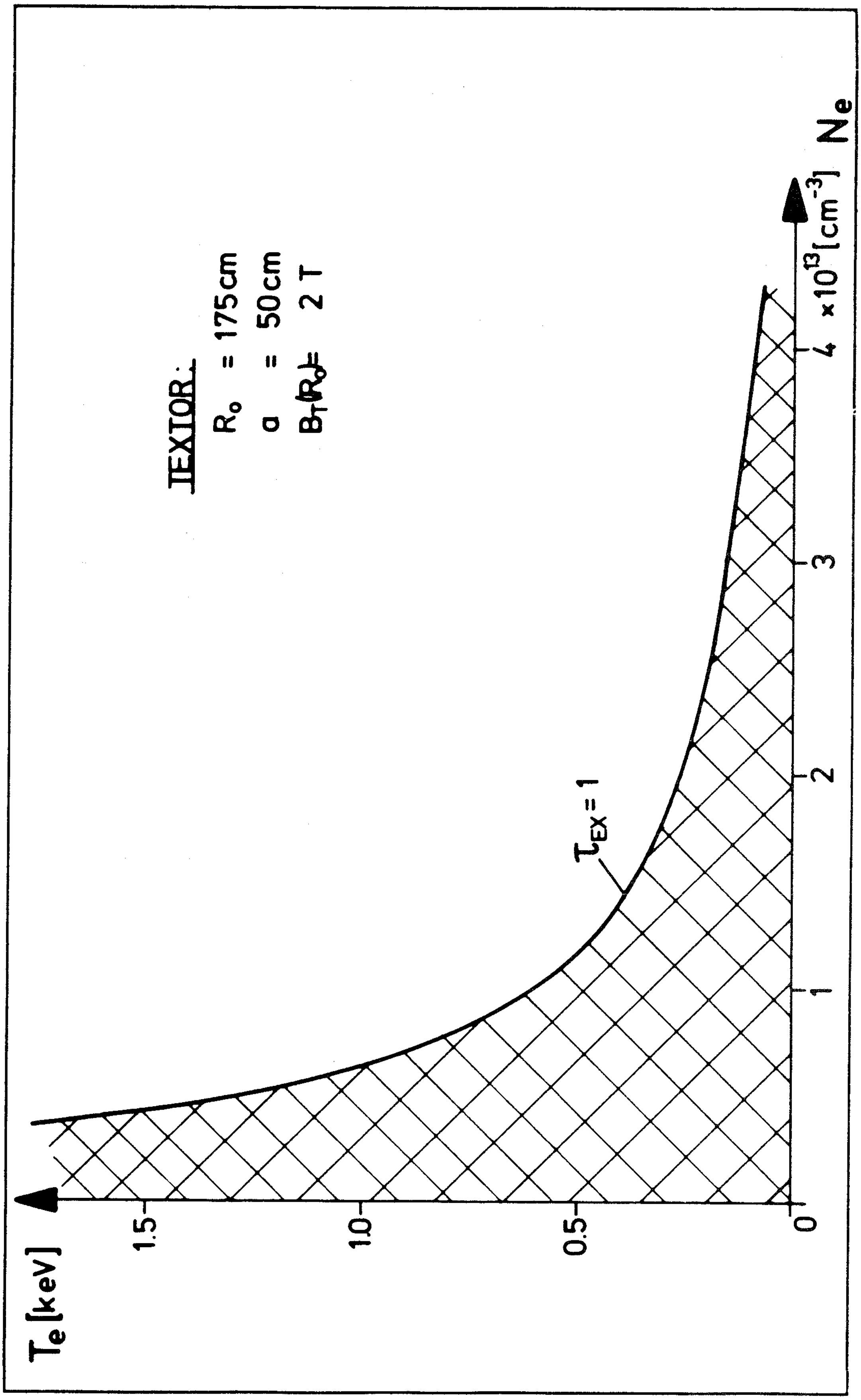

Fig. 4 The optical thickness $\tau_2^{(x)} = 1$ as a function of electron density and temperature. The condition $\tau_2^{(x)} > 1$ lies outside the shaded area.

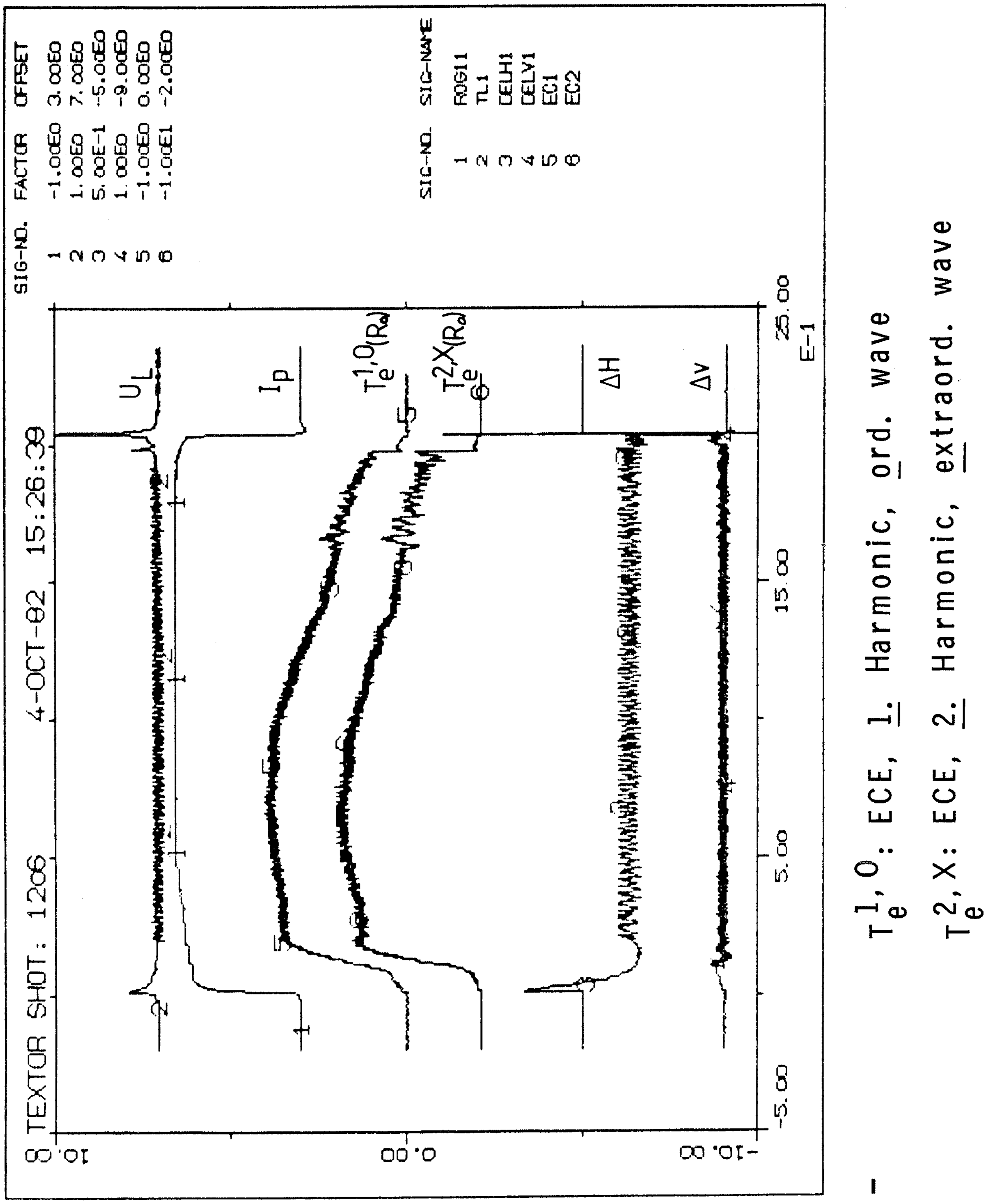

Fig. 8 Comparison of the radiometric signals for the first harmonic $T_{e1}^{(o)}$ and the second harmonic $T_{e2}^{(x)}$; Δ_H horizontal and Δ_v vertical position of the plasma.

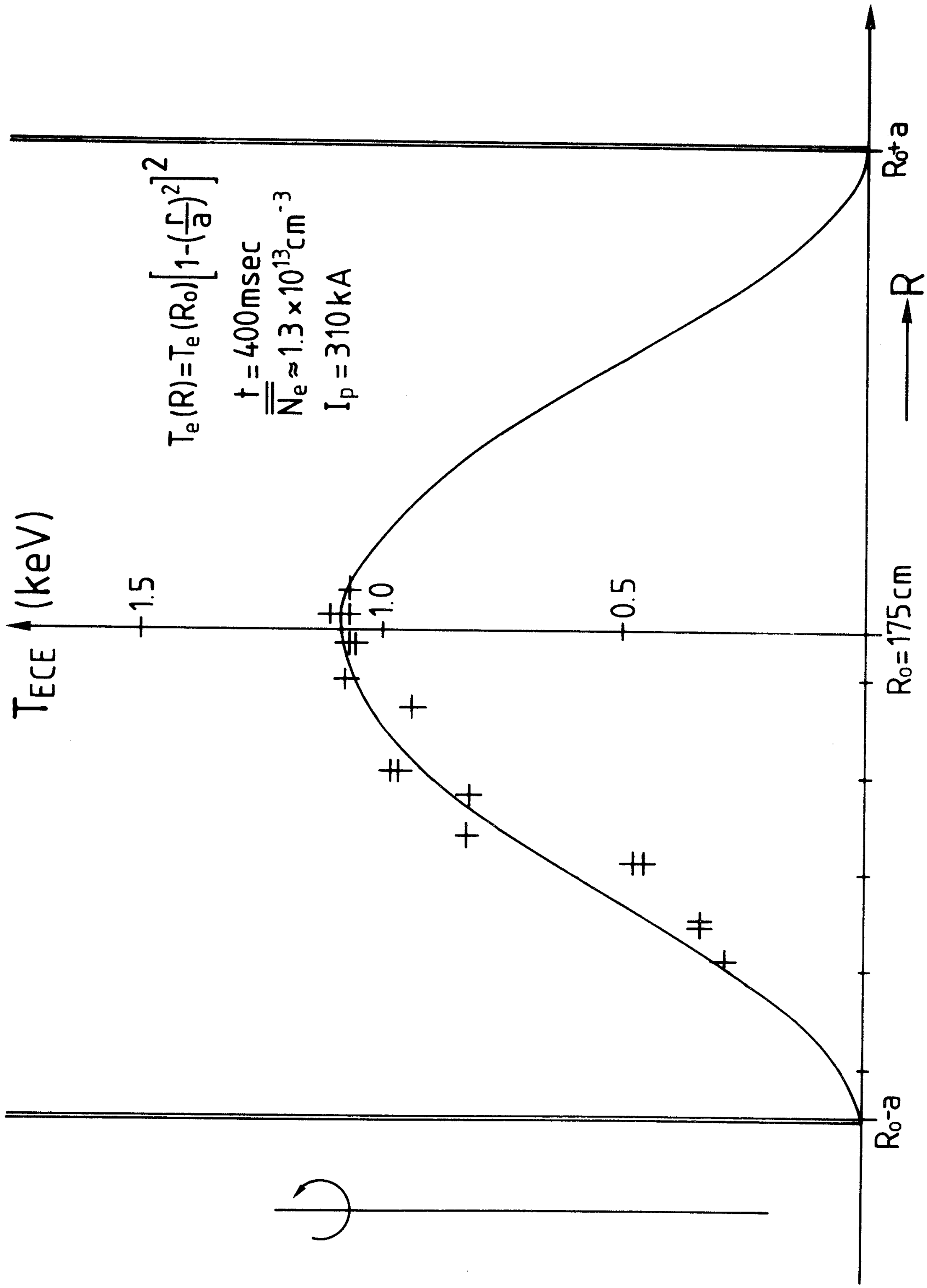

Fig. 9 Electron temperature profile measurement obtained by a variation of the toroidal magnetic field using the first harmonic receiver.

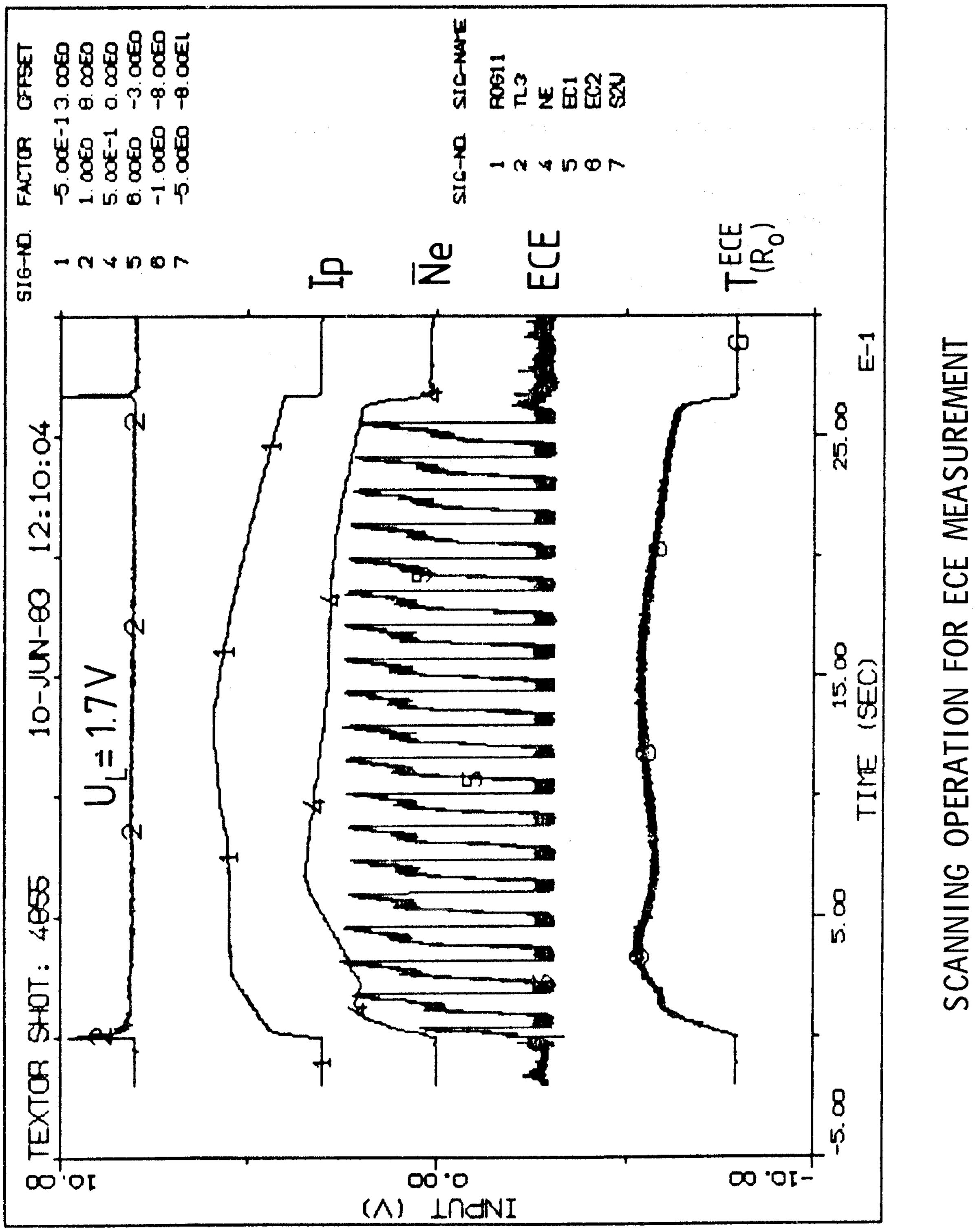

Fig. 10 ECE-recording for a TEXTOR discharge (# 4855) with the scanning and fixed frequency radiometer. The scan period used here was 100 msec.

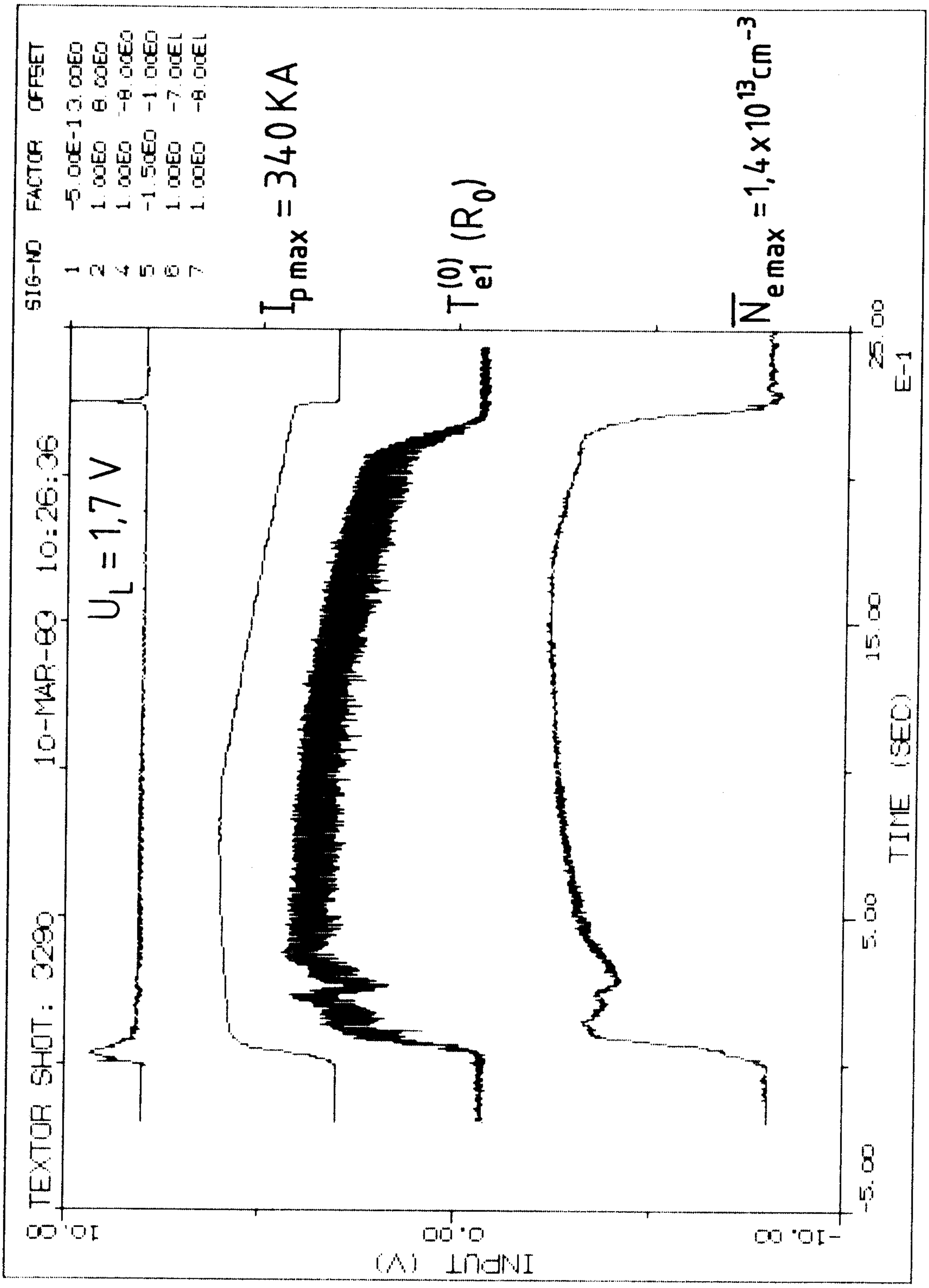

Fig. 12 TEXTOR discharge with internal disruptions and sawtooth modulation of ECE.

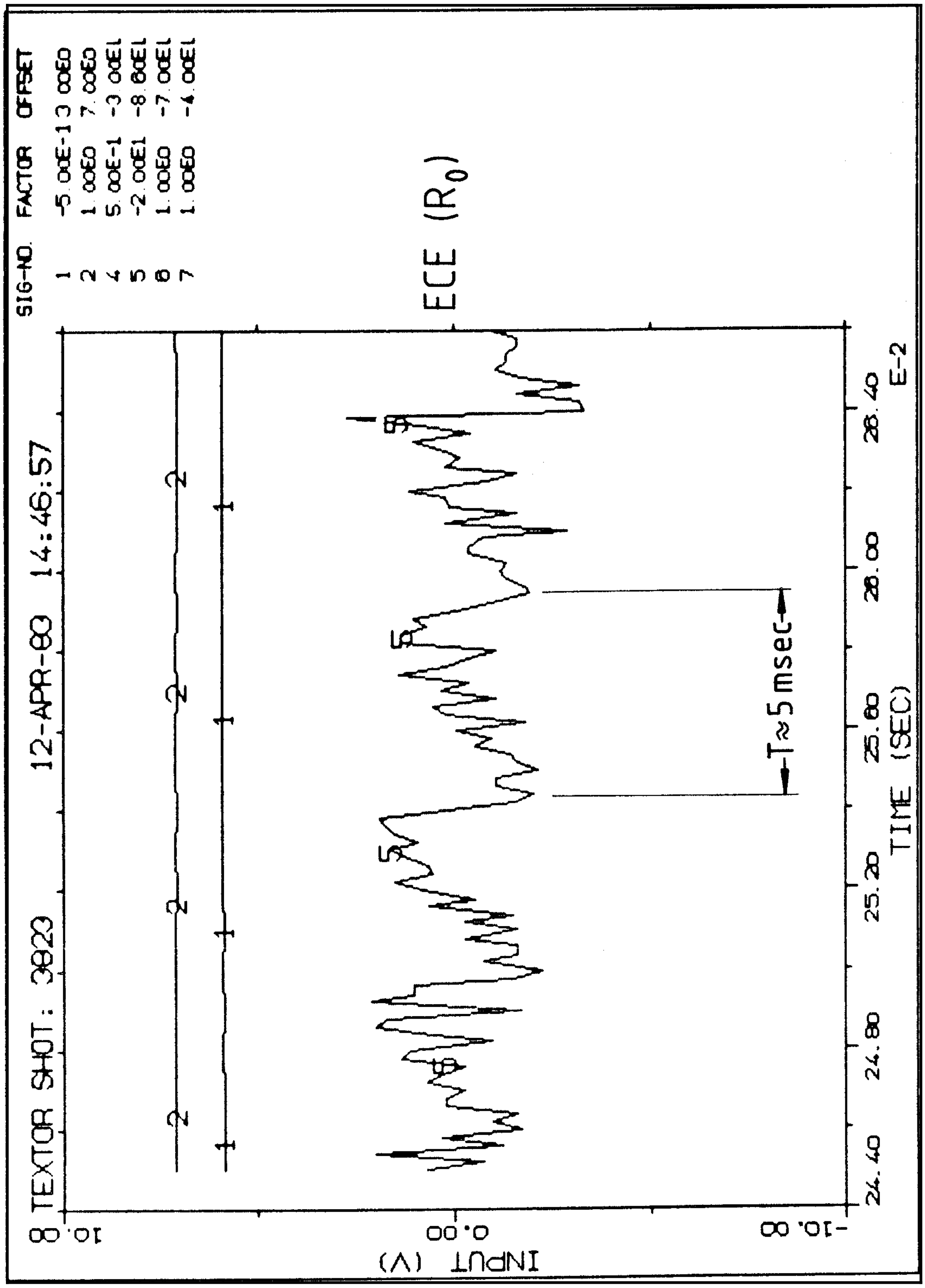

Fig. 13 Sawtooth oscillations enlarged showing a hyperfine structure in ECE. The oscillation period is dependent on electron density.

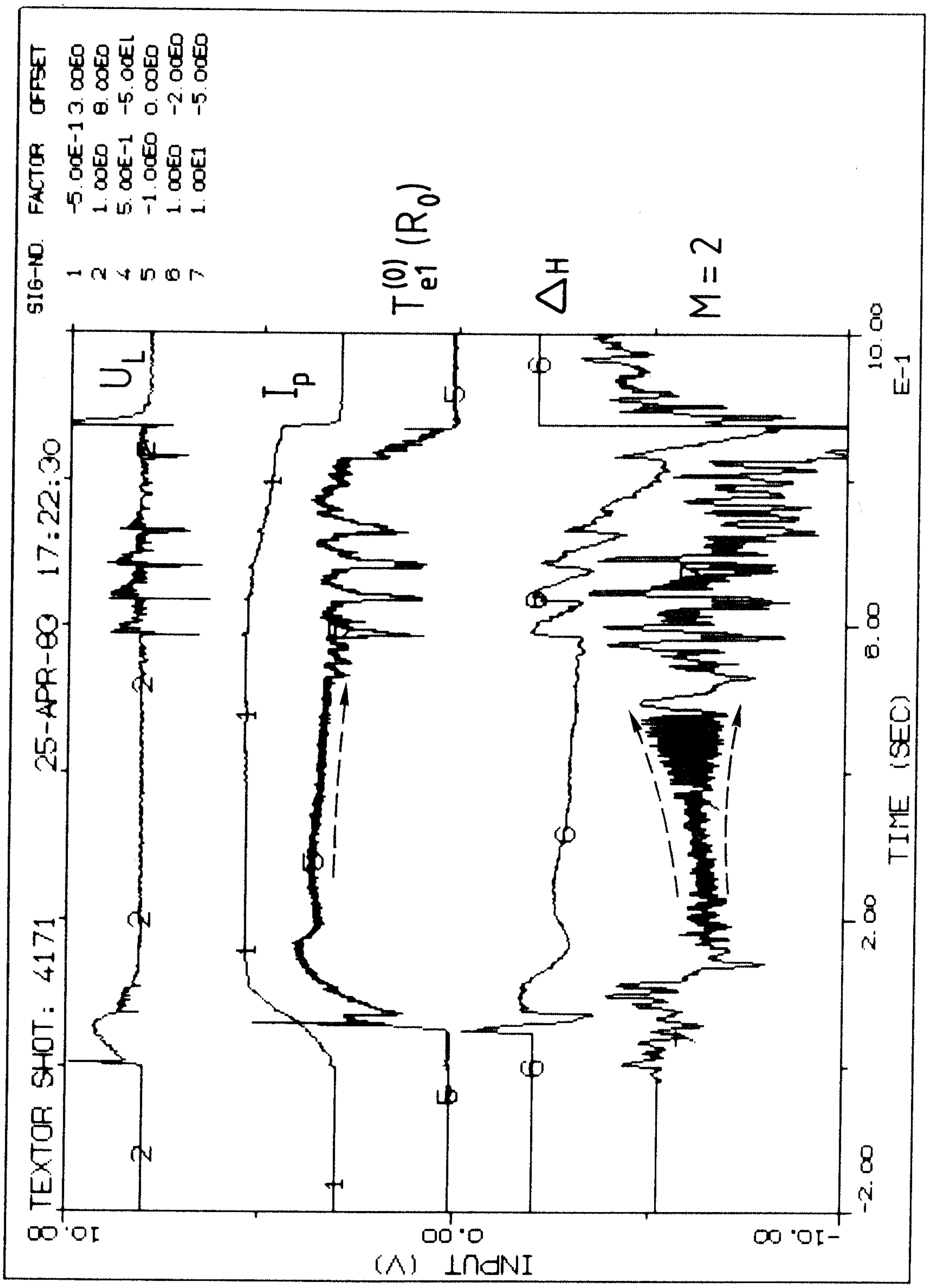

Fig. 14 TEXTOR discharge with M = 2 mode activity. Decaying ECE radiation, precursors to minor disruptions and strong dips in ECE at major disruptions.

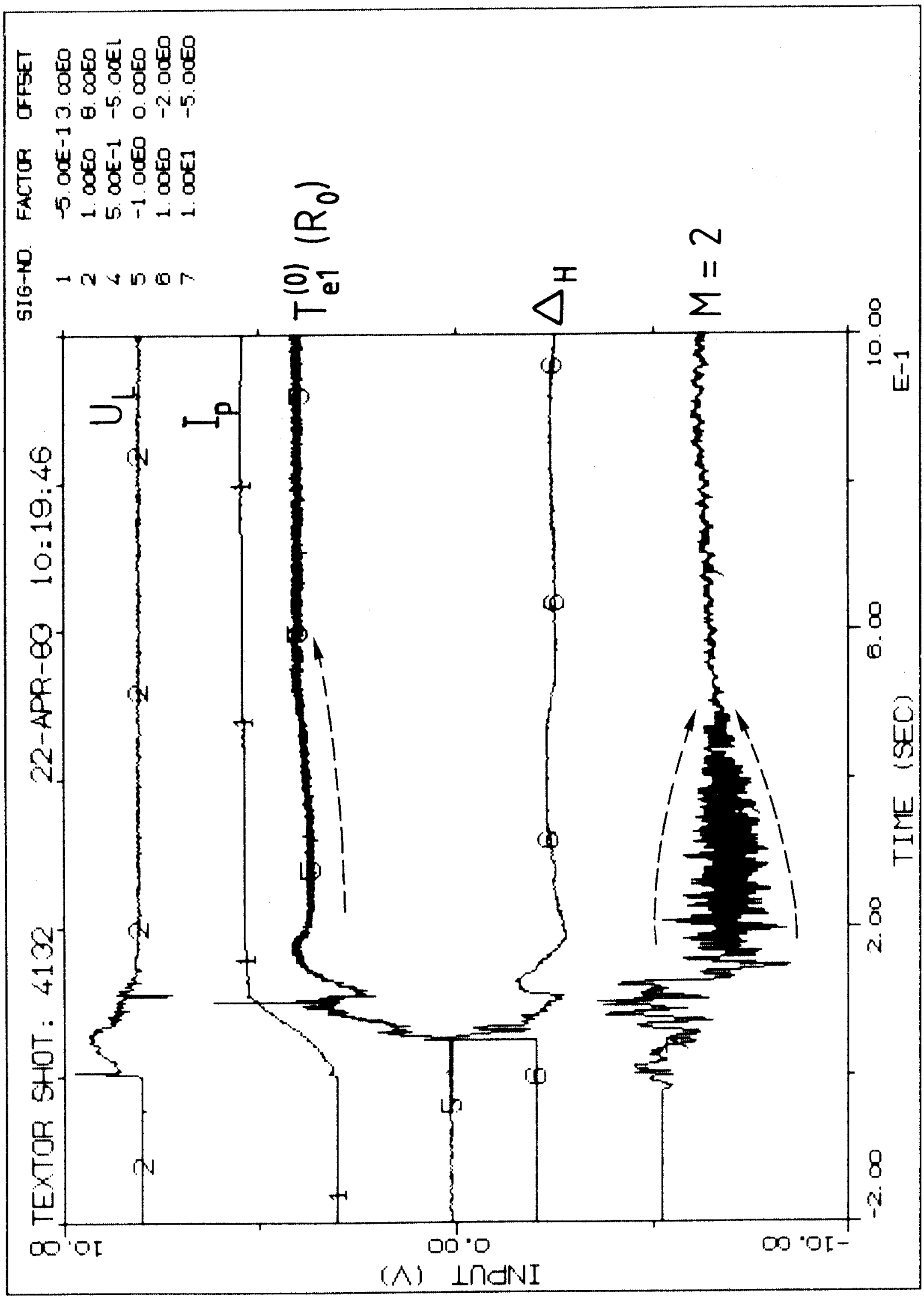

Fig. 15 TEXTOR discharge with initial M = 2 mode activity. ECE radiation recovers after choking of the M = 2 mode.

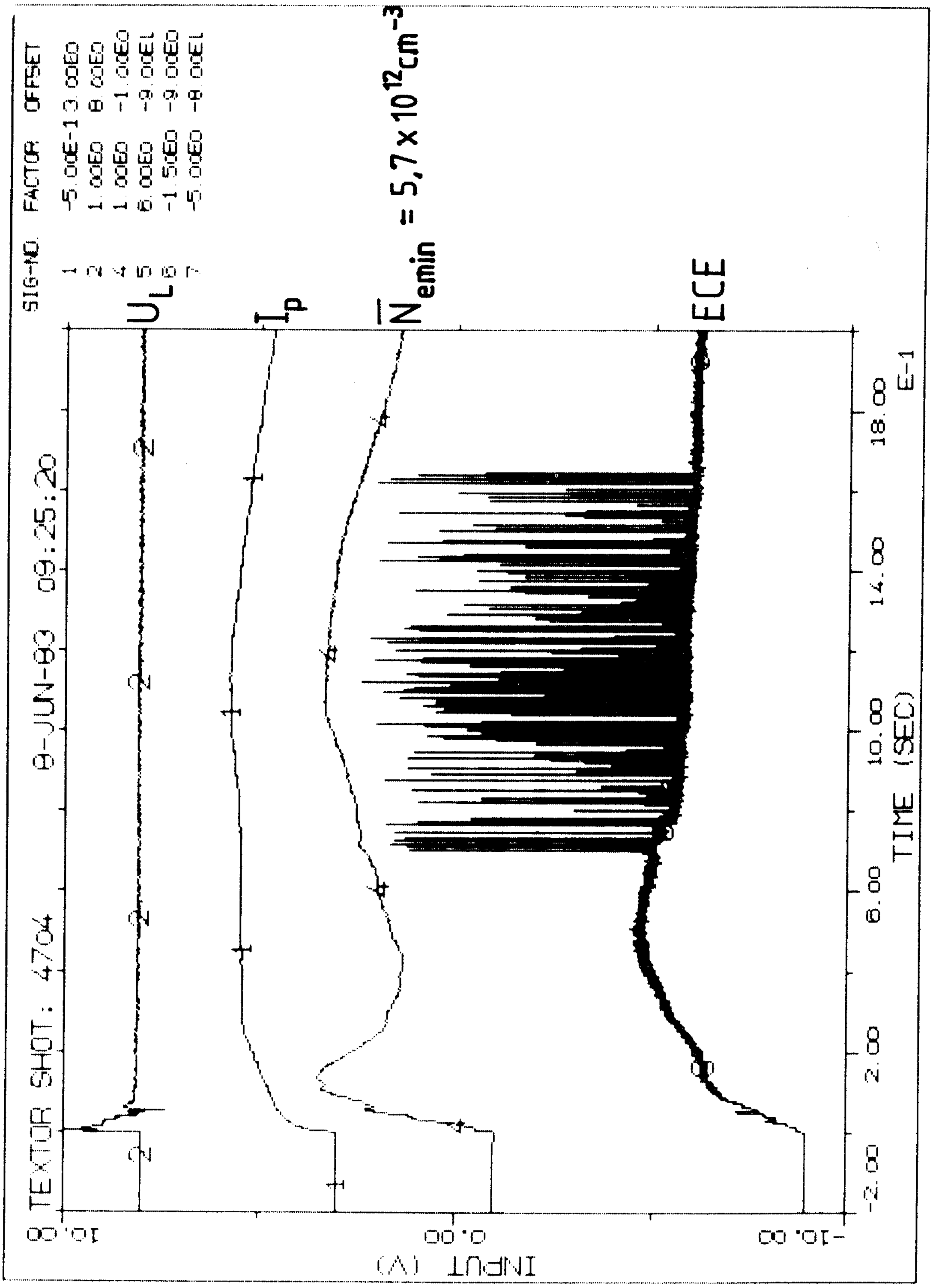

Fig. 16 Nonthermal ECE-radiation superimposed on the thermal emission, observed after low electron density operation of the TEXTOR experiment.

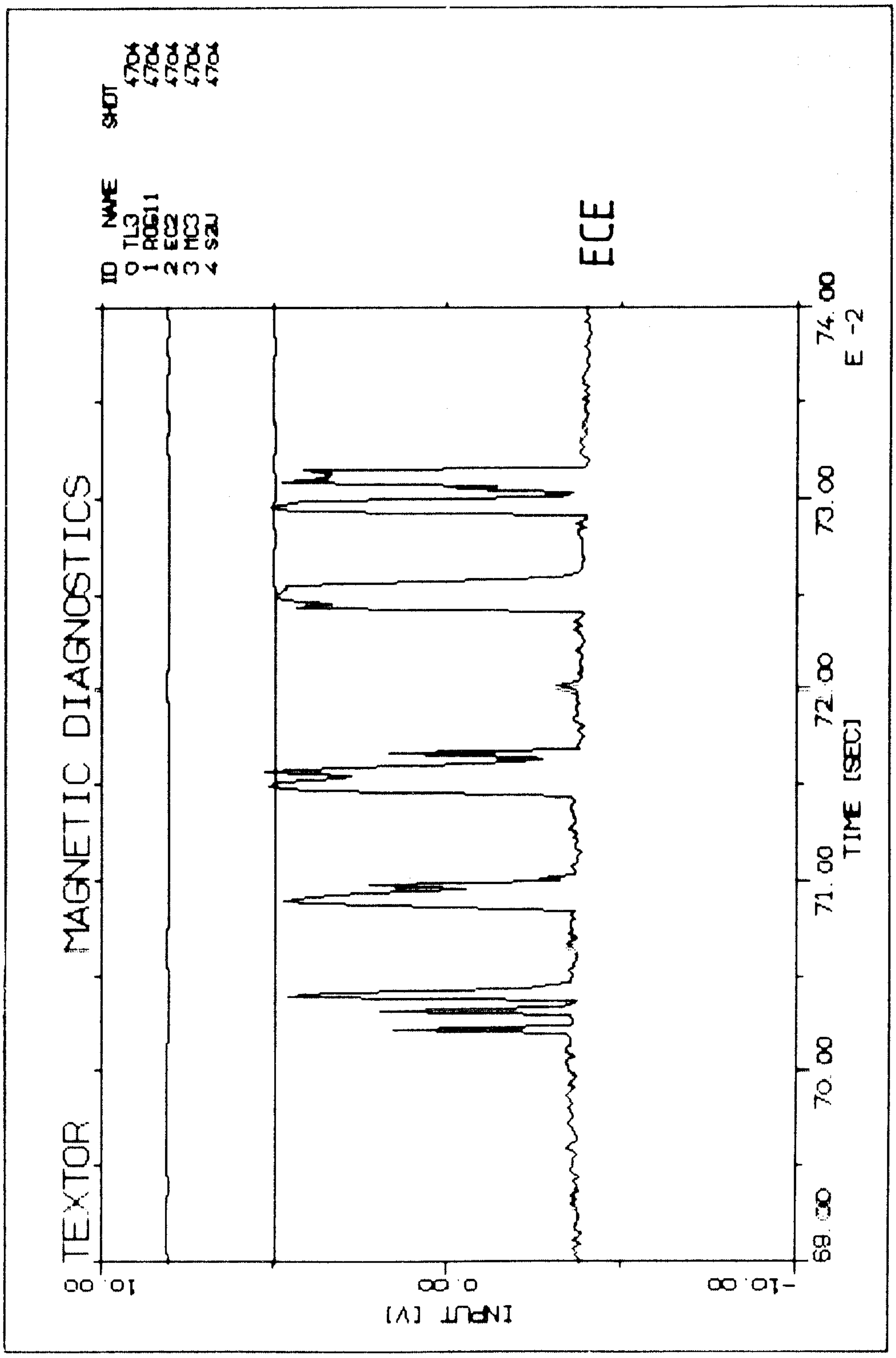

Fig. 17 Shape of the radiation spikes superimposed on the continuous signal of ECE.